Delft University of Technology

Effectiveness of Wide-Area Selective Damping Control in Power Systems with High Shares of Power Electronics

Vit Suntar, Jan; Rueda Torres, Jose L.; Stefanov, Alexandru; Kruimer, Bas; Berenschot, Coen; Prka, Lino

Citation (APA)
Vit Suntar, J., Rueda Torres, J. L., Stefanov, A., Kruimer, B., Berenschot, C., & Prka, L. (2022). Effectiveness of Wide-Area Selective Damping Control in Power Systems with High Shares of Power Electronics. In *IECON 2022 - 48th Annual Conference of the IEEE Industrial Electronics Society* (IECON Proceedings (Industrial Electronics Conference); Vol. 2022-October). IEEE. https://doi.org/10.1109/IECON49645.2022.9968631

Important note
To cite this publication, please use the final published version (if applicable).
Please check the document version above.

Effectiveness of Wide-Area Selective Damping Control in Power Systems with High Shares of Power Electronics

Jan Vit Suntar
Digital System Operations
DNV Energy Systems
Arnhem, the Netherlands
Janvit.Suntar@dnv.com

Jose L. Rueda Torres
Intelligent Electrical Power Grids
Delft University of Technology
Delft, the Netherlands
J.L.RuedaTorres@tudelft.nl

Alexandru Stefanov
Intelligent Electrical Power Grids
Delft University of Technology
Delft, the Netherlands
A.I.Stefanov@tudelft.nl

Bas Kruimer
Digital System Operations
DNV Energy Systems
Arnhem, the Netherlands
Bas.Kruimer@dnv.com

Coen Berenschot
Digital System Operations
DNV Energy Systems
Arnhem, the Netherlands
Coen.Berenschot@dnv.com

Lino Prka
Digital System Operations
DNV Energy Systems
Arnhem, the Netherlands
Lino.Prka@dnv.com

Abstract— **A large contribution to the total share of electricity generated in European power grid will come from renewable sources of energy soon due to European initiative to become carbon neutral. Renewable Energy Sources (RES) are connected to the grid with Power Electronic (PE) devices, which, if not modelled correctly, provide low confidence in the assessment of the overall system stability. The aim of the paper is twofold; firstly, to evaluate the impacts of Wide Area Monitoring System (WAMS) on grid-forming control with Direct Voltage Control (DVC) and Virtual Synchronous Machine (VSM). Secondly, to perform Modal / Eigenvalue analysis to evaluate the effect of WAMS on selective damping. Modal analysis will be conducted and will serve as a base for calculating matrices B and C. Left and right eigenvectors will enable determination of Controllability and Observability Indices. Damping controller is designed to receive three signals from Phasor Measurement Units (PMUs) and feed the reference signal to the high impact generator. System studied is a modified IEEE 39 New England Bus with two synchronous generators and eight RES. Activation of the damping controllers showed significant improvements in time-domain simulations on overall damping and Eigenvalue confirmed the results by studying the damping ratios of critical modes.**

Keywords— WAMS, Direct Voltage Control, PE Interfaced Generation, Selective Damping Control

I. INTRODUCTION

One of the main points of interest for the future power grids is a contribution of an onshore system with a large participation of RES to the overall electricity generation. Contribution of a wind power generation to the overall electricity generation is increasing rapidly and has a potential to reach 70% to 80%. Grid-forming control will have to be implemented to ensure stabilizing of the grid following a disturbance [1]. Another significant challenge of heavily RES penetrated power system is decrease of total inertia in the system and reduced total damping of the power system [2].

This paper will take into consideration already developed technology, such as Wide Area Monitoring System, grid-forming control (Direct Voltage Control and Virtual Synchronous Machine) and grid-following control. The impacts of WAMS based mitigation solutions will be studied on rotor-angle stability with total of 20% of synchronous generated power. Grid-forming control concept has been heavily described in literature, due to its ability of generating its own set points. A concept of direct power control, which has an ability of directly regulating active and reactive power, has been researched in [3]. Furthermore, method of Virtual Oscillator Control with an ability of synchronizing and controlling inverters has been studied in [4] and a method of direct voltage control has an ability of keeping voltage in acceptable limits was studied in [5]. Identification of critical OMs has been described in literature as a technique of evaluating the system and investigating parameters such as damping ratios, modes of oscillation and eigenvalues [6].

It has been discussed and demonstrated in the literature how different grid-forming controllers successfully enhance system stability when a single type of the controller is present. Benefits of using forming controllers have been highlighted in cases when majority of power is generated by renewable sources of energy or when the system enters the islanding mode. However, literature lacks insight into case studies when multiple types of gird-forming controllers is used in the system at the same time. A study of impact on overall damping of the system must be carried out in order to visualize and observe any drawback or enhancements of using different types of controllers. Analysis examines whether interaction between newly introduced controllers impacts overall system damping. Additionally, it examines whether benefits of adding new controllers are visible by implementing controllers without additional customization or should controllers rather be examined, and parameters adapted to add the desired value.

Literature explains several input and output signal selection methods to determine proper input and output signals for wide area damping controllers. A method based on Geometric Measures of Controllability and Observability is discussed in [7]. Furthermore, Residue Method and Hankel Singular Value Method are explained in [8]. Previously developed method for input and output signal selection were designed for system with 100% synchronous generation. These methods thereafter must be modified in order to be able to obtain information regarding input and output signals in systems with mainly power converters. Modification of previously developed methodology is necessary for

identification of highest controllability indices and to locate the generators which have the highest damping effect.

Work carried out in this project build upon findings from Horizon 2020 MIGRATE project, where it has been identified that grid-following control enables 60% penetration of RES. It has been also stated that grid-forming control enables higher penetration of RES, sometimes even up to 100% of RES penetration. Importance of enhanced monitoring of detection of oscillatory instabilities has been studied during work package 2 [9].

This paper considers the controllability and stabilizing aspect of the system analysis; hence it focuses on controller aspect and not as much towards PMUs and input signal selection. Due to the design of Direct Voltage Controller (DVC), signal fed into the controller was voltage magnitude. The preferred option would be rotor angle since it would give more information regarding the state of the system. It has been determined that such WAMS structure satisfies objectives of the paper. Methodology adopted in this paper starts by examining the standardized IEEE 39 New England Test System. Synchronous generators have been replaced with type 4 wind turbines to firstly test findings from MIGRATE project. Additionally, wind turbines have been designed to have the ability to either activate grid-following control or grid-forming control; depending on what is the objective of the case study. Finally, there is an option to activate two different grid-forming controllers for different wind turbines at the same time to study a more realistic scenario. Addition of grid-forming controllers with a stabilizing signal fed to the controller has proven beneficial which was visible in time-domain simulations. Positive effect was observed on the rotor angle stability of the remaining synchronous generators. Eigenvalue analysis results sometimes do not follow previous observations. Such behavior can be assigned to an introduction of newly added controllers. Benefits of using grid-forming controllers when enhanced by supplementary damping controllers have been proven, however more research must be done to really understand behavior and interaction of controllers.

The remaining of the paper is organized as follows. Section II gives information about the selective wide area damping controller, section III summarizes relevant case studies and simulation results, and section IV concludes the main findings of the project.

II. SELECTIVE WIDE AREA DAMPING CONTROLLER

A. Control Strategies

Power Electronic (PE) devices will be adopted in the future in high voltage transmission grid, where synchronous generation will be replaced by control strategies. These control strategies will either be grid-forming control or grid-following control and main advantage of a grid-forming controller is its ability to form its own frequency and voltage. A conventional grid-following control applied in a power grid with high penetration of PE interfaced generation is a current control. This paper focuses on the impact of introducing grid-forming controllers to the system, with studying Direct Voltage Control and Virtual Synchronous Machine concepts.

1) Direct Voltage Control

Reactive power control structure implemented in DVC is represented by figure 1. Slow global Var control's response time is in range of couple of seconds and up to 30 seconds

[10], and VQ droop block is used to set a reactive power reference signal as an input for a PI block to generate the voltage signal.
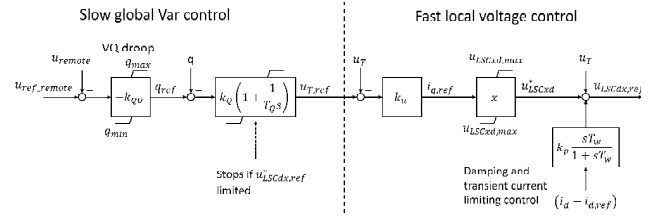

Figure 1 DVC reactive power control [10]

A fast local voltage control with proportional characteristics acts for events that require a faster response. The implementation of limiting control allows a selective damping and replaces the proportional component [10]. D-component is determined after an addition of controlled terminal voltage and the reactive current is therefore removed from a control scheme. This eliminates a possibility of integrator windup during an event, which causes a split of the system [10].

Figure 2 shows an active power control structure with corresponding elements. The function of a fast frequency control is set to react when frequency crosses the threshold value [10]. Voltage dependent active power reduction is used to improve the transient stability. The power reference power set point is lowered during the fault, which compensates converter's inability to inject reactive power into the system. The power injected is adjusted based on the terminal voltage of the converter.
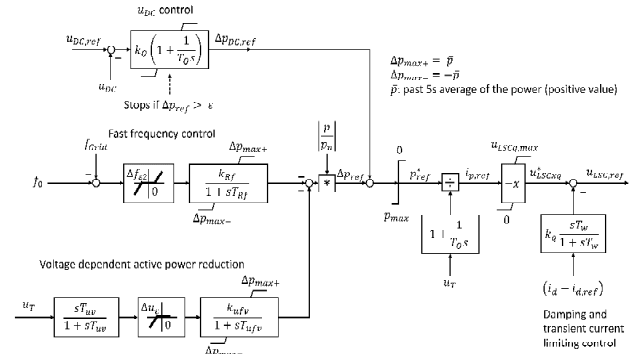

Figure 2 DVC active power control [10]

The active power injected into the network is represented by an equation 1 [10].

$$p = u_t i_P = -u_t \frac{u_{Cq}}{x} \tag{1}$$

where p represents active power, u_t represents terminal voltage, u_{C_q} represents q-component of the converter voltage and x represents the reactance.

2) Virtual Synchronous Machine

Virtual synchronous machine has an ability to provide virtual inertia and mimic the behavior of a synchronous machine. Mechanical inertia is emulated and can be represented by a swing equation. An internal dynamics and behavior of a VSM can be represented by a SG per unit balance in the Laplace domain [11]:

$$T_a s \omega_{VSM} \approx p_0 - p_{el} - D_p(\omega_{VSM} - \omega_g) \tag{2}$$

where a time constant Ta represents the rotor angle; hence it can also be written as 2H, p_0 and p_{el} represent the power reference and power output respectively, and D_p is a damping coefficient. Equation also represents rotating speed of VSM, ω_{vsm} and grid frequency, ω_g. Since this controller is mainly used in weak grids, the grid frequency ω_g will become a frequency reference provided by an additional controller. VSM provides a voltage angle θ_v as an output, however the voltage amplitude must be provided by a separate reactive power controller. The block diagram of a grid-forming part of a VSM controller is shown in figure 3 [12].
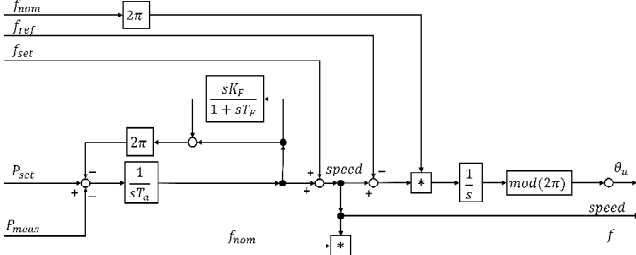

Figure 3 Grid-forming block of the virtual synchronous machine [12]

B. Wide Area Damping Controller

The design of a WADC is shown in figure 4 and it has a similar design as a Power System Stabilizer (PSS) block, since they both have an objective to enhance damping of oscillations in the system. There are three inputs to the wide area damping controller (u_1, u_2, u_3), as visible in the figure, which are measurements collected by PMUs. u_1 measurement is a signal collected from the bus with the highest controllability index, u_2 measurements is collected from the bus with the second highest observability index and u_3 measurement is collected from the bus with the third highest observability index. It has been decided that three inputs to a damping controller will provide enough information from the critical parts of the system to validate the controllability. Input signals have a corresponding gain block to enable the optimization algorithm to assign different "weight" to the specific input signal. Other blocks present in the design are a washout filter and two lead/ lag compensation blocks. Washout filter removes the undesired low-frequencies and lead/ lag compensation blocks improve the frequency response.
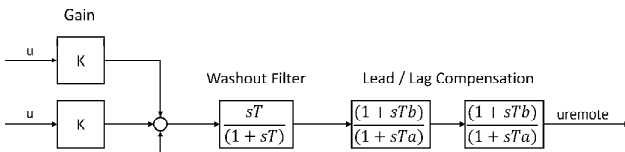

Figure 4 Blocks used in designing the wide area damping controller

The WAD blocks and their corresponding parameters that were used in the WADC are shown in the table 1. Initial values assigned to the parameters were based and matched to the values used for the Power System Stabilizers in the test system [13]. Initial values will eventually be adjusted with optimization algorithm called Particle Swarm Optimization (PSO) to have the highest effect on damping.

TABLE I.   DAMPING CONTROLLER PARAMETERS

Symbol	Value	Symbol	Value
Kpss1 [pu]	1	T1 [s]	5
Kpss2 [pu]	1	T2 [s]	0.4
Kpss3 [pu]	1	T3 [s]	1
Tw [s]	10	T4 [s]	0.1

C. Input and Output Signal Selection Method

The main technique for determining critical modes, damping ratios and frequencies will be Modal or Eigenvalue analysis. It will additionally be used for input and output signal selection for determining locations of PMUs and WADCs. The theory behind eigenvalue and eigenvector dependency on matrix A is represented by equation 3, 4 [14]:

$$(A - \lambda_i I)v_i = 0 \qquad (3)$$

$$\omega_i^T (A - \lambda_i I) = 0 \qquad (4)$$

where v_i represent the right eigenvectors and ω_i represent the left eigenvectors associated with the eigenvalue λ_i and A is a matrix A, which depend on system parameters.

In order to obtain the expression, which is useful for this project, equations 3 and 4 have to be differentiated with respect to parameter K and the obtained expression then needs to be multiplied by left eigenvector ω_i^T. An assumption taken into consideration is that the left and right eigenvectors are orthogonal ($\omega_i^T v_i = 1$). The final expression is then:

$$\frac{\partial \lambda_i}{\partial K} = \omega_i^T \frac{\partial A}{\partial K} v_i \qquad (5)$$

It is assumed that by following the analysis explained in [14], only a handful of damping controllers are needed in to achieve desired level of damping and system stability. A controllability index (CI) and an observability index (OI) are expressed by equations:

$$CI_l = \frac{MC_l}{\max_{l \in L} MC_l} \qquad (6)$$

$$OI_\delta = \frac{MO_\delta}{\max_{\delta \in \Delta} MO_\delta} \qquad (7)$$

where CI is a controllability index, MC is the mode controllability, OI is an observability index and MO is the mode observability. Controllability and observability indices are obtained by normalizing the mode controllability (MC) and mode observability (MO).

$$|\lambda_i'| = |\omega_i^T B_a| \cdot |H(\lambda_I)'| \cdot |C_a v_i| \qquad (8)$$

where $|\omega_i^T B_a|$ represent the mode controllability (MC) of mode i and $|C_a v_i|$ represent the mode observability (MO) of mode i. More details about the derivation can be found in the reference [14].

Important to point out is that matrix A is available as an output of the Modal analysis, while, matrix B, matrix C and matrix D are not available as the output. This is because they depend on user definition. A flow chart which was followed to determine best locations for PMUs and for WADCs can be found in [14].

1) Matrix B Calculation and Controllability Index
Controllability indices are obtained by considering a matrix B and a left eigenvector associated with previously

selected eigenvalue. Eigenvalue of interest for this project is the one associated with the inter-area mode of oscillation [14]. Task is executed by locating the desired eigenvalue based on setting the range of the imaginary part. Real and imaginary part of the left eigenvector are used to get the magnitude of the mode controllability, which are normalized to obtain controllability indices.

2) Matrix C Calculation and Observability Index

Observability indices are obtained similarly to controllability indices, except this time matrix C and the right eigenvector are considered. The difference from the procedure explained before is that in this case there is only one output per row when matrix C is multiplied with the right eigenvector [14]. This is due to a matrix C only having one nonzero value per row, which is the only one that will give the nonzero output. The obtained values are observability mode, which are normalized to obtain observability indices.

III. CASE STUDIES & SIMULATION RESULTS

Software used in this research is DIgSILENT PowerFactory 2021 SP1. The simulations were run in a PC with an Intel Core i7 processor (2.20 GHz) and 16 GB RAM running Windows 10. The average computing time to run 20 s of RMS simulation, with an integration time step of 0.01 s, was approximately 5 s.

A. Disturbances

The effectiveness of WAMS will be evaluated in time-domain by observing the system response to a small disturbance. Results will be compared to a large disturbance and differences will be highlighted. The small disturbance is modelled as a load event at time = 1 s, with an increase of active power demand of load 15 by 15%. The large disturbance is a short circuit event on the Line 16-24 at time = 1 s. The short circuit event is cleared after 0.15 seconds at t = 1.15 s. The short circuit has the impedance of 1.5 Ohm resistance and 15 Ohm reactance.

B. Modified IEEE 39 New England Test System

IEEE 39-Bus New England Test System was taken as a starting point. A part of the single-line diagram of the system is shown in figure 5 to point out the modifications made on power plants 5, 6, and 7. Test system was modified by using library models and the DSL programming language of PowerFactory to include PE devices and WAMS functionality with PMUs and WADC.
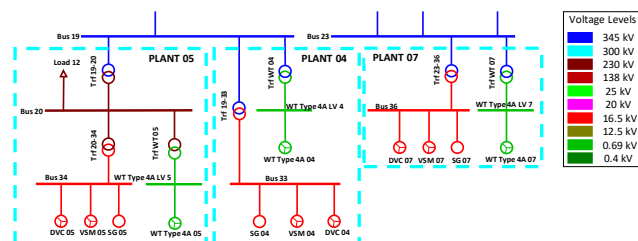

Figure 5 One Line diagram of plant 05, 04 and 07 of modified system

In the modified system, the units G01 and G02 constitute the two remaining synchronous generators that will remain in the system. The rest of the power generation is represented by wind power generation, which can work under grid-following or grid-forming control. The first key case study carried out is 80% penetration of wind generation with three wide area

damping controllers. The second key case study is the 80% penetration of wind generation with two different grid-forming controllers as well as grid-following control deployed.

C. Case Studies

1) WAMS with 2 SGs, 8 DVCs and 3 WADCs

This case study focuses on impact of 80% penetration of RES with grid-forming controllers, while only 30% of them have a WADC. MIGRATE project has proven that grid-following control can withstand disturbances for 60% penetration of RES. The first task was then to prove whether grid-forming control will enable higher penetration levels of RES. A total of 30% of power generation has WADCs associated and input and output signal selection method is executed for determining best locations of PMUs and WADCs. Input and output method is explained in section II part C. Analysis has determined that the power plants which should receive the stabilizing signal are Power Plant 7, Power Plant 6 and Power Plant 4 based on calculated Controllability Indices (CI). On the other hand, analysis has determined that the highest Observability Indices (OI) are found for Bus 34, Bus 36 and Bus 33 and measurements from these buses will serve as an input signal.

The RMS simulation was carried out when WADCs were disables and results were compared to the situation when three WADC were enabled. Figure 6 shows the time-domain response of generators G01 and G02 after being subjected to the load event on the line 15 (blue lines in the figure). In the same figure a time-domain response of the short circuit is also plotted for the reference (green lines in the figure). The oscillations visible in the figure occur with the introduction of an event. From the figure it is visible that in the case without WADCs the oscillations decay slowly and are not able to damp out like in the case with WADCs. Oscillations are not able to damp out due to lack of inertia and grid-forming controllers are able to enhance damping through their control loops.
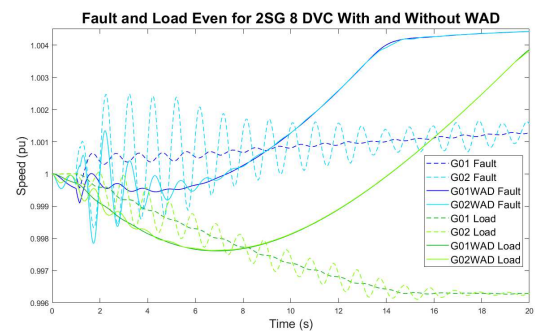
Figure 6 A response of a system to a fault event and load event

WADC parameters were tuned by using a Particle Swarm Optimization [15]. Table 2 collects initial and tuned values determined for the gain block of the three input signals.

TABLE II.   INITIAL AND TUNED WAD PARAMETERS

Symbol	Initial	WAD 04	WAD 06	WAD 07
Kpss1 [pu]	1	0.475	4.234	2.260
Kpss1 [pu]	1	0.838	0.097	0.980
Kpss1 [pu]	1	3.790	3.600	1.549

The optimization problem conducted in this project is a bound constrained signal objective optimization problem with an objective function defined with an equation 9 [15]:

$$e = \int_{t_0}^{t_{max}} \sum_{n=1}^{n} \left|\left(m_i(t) - c_i(t)\right)w_i\right|^p dt \qquad (9)$$

where m_i is a measured response, c_i is a simulated response, w_i is a weighting factor and p is power. The bound constraints with initial values are shown in table 3. These bounds are set up to limit the possibilities available for determining parameter values. It serves as a pool of available parameters which optimization tool can use to find the overall best solution. The inequality defining the bound constants is:

$$x_{min} \leq x \leq x_{max} \qquad (10)$$

Such bounds were determined based on standard limit range of the parameters for PSS found in literature [16] and adjusted for the initial values of the parameters. Experimental work was done to determine the impact of the parameters when the values are moved out of the range, and it has been identified that these bounds return a feasible result.

TABLE III.   WADC LOWER AND UPPER BOUNDS

Symbol	Initial	Lower Lim	Upper Lim
Kpss1 [pu]	1	0	5
Kpss1 [pu]	1	0	5
Kpss1 [pu]	1	0	5

Table 4 collects critical modes without a damping controller, which fall into range of local oscillatory modes (frequency around 1.0 Hz). Local mode of G2 oscillates against the system with a frequency of around 1.0 Hz. Eigenvalue analysis has been executed to determine the eigenvalues, damping ratios and damped frequencies of the critical modes of oscillation.

TABLE IV.   MODAL ANALYSIS RESULTS WITHOUT DAMPING CONTROLLER

Modes	Eigenvalues	Frequency	Damp. Ratio
Units	[1/s +j rad/s]	Hz	-
Mode 1	-0.509 ± j 6.021	0.958	0.084
Mode 2	-2.491 ± j 8.488	1.351	0.282

Two critical modes of oscillation were identified for a case with a damping controller and are collected in table 5. The listed modes fall in a range of local modes of electro-mechanical oscillation with damped frequency around 1.0 Hz. By comparing the results from both tables one can notice a slight decrease in damping ratio for Mode 1 and an improvement in damping ratio for Mode 2. Eigenvalue analysis might not show the desired positive impact WADCs have on damping enhancement of critical modes, which presents an opportunity for future research.

TABLE V.   MODAL ANALYSIS RESULTS WITH DAMPING CONTROLLER

Modes	Eigenvalues	Frequency	Damp. Ratio
Units	[1/s +j rad/s]	Hz	-
Mode 1	-0.460 ± j 6.386	0.972	0.079
Mode 2	-6.121 ± j 9.910	1.433	0.356

2) WAMS with 2 Synchronous Generators, 3 DVC, 1VSM and 4 WT with Grid-Following Control

The second use case studied consists of two synchronous generators and 80% PE penetration. There is a total of 40% of grid-forming control as well as 40% of grid-following control. This case is relevant because it is representing a realistic scenario, where the existing grid-following control will not be replaced in the future with grid-forming control. Another modification made was an introduction of a different grid-forming control (VSM). The intent was to either observe benefits of adding a new type of control or learn from the drawbacks. Just like in the previous case, three PMUs will feed three stabilizing signals into WADC and there will be a total of three DVC in the system. Due to out of the box design of the controllers used in this project, DVC is the only controller which is able to receive the stabilizing signal; meaning that VSM is not able to receive the stabilizing signal. OIs were recalculated for this case and highest values for OI are found for Bus 36, Bus 35 and Bus 33. Similarly, CIs have been recalculated and the highest values were identified for Power Plant 7, Power Plant 6 and Power Plant 4.

Time domain simulation results demonstrated in figure 7 highlight the impact of WAMS on damping following the small and large disturbance. In both cases the oscillations are able to damp out around 8 seconds after the disturbance, which is the case with WADCs. This is due to introduction of the VSM, which is able to replace lack inertia in the system by emulating the inertia usually provided by rotational part of the machine.
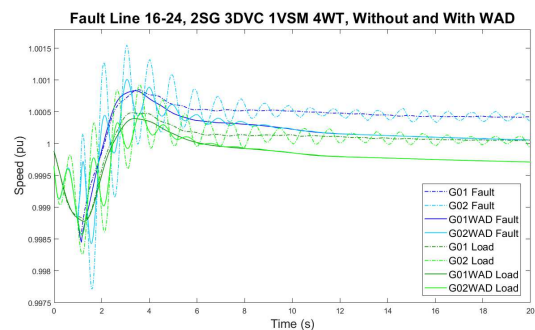

Figure 7 A response of the system to a fault event on Line 16-24

Table 6 shows the result of the Modal analysis conducted for the system without WADC and corresponding critical modes of oscillation are presented. Mode 1 has damping lower than 10%, however the next critical mode identified (Mode 2) has a damping ratio above 50%. It can also be seen that there are only local modes of oscillations in the system.

TABLE VI.   MODAL ANALYSIS RESULTS WITHOUT DAMPING CONTROLLER

Modes	Eigenvalues	Frequency	Damp. Ratio
Units	[1/s +j rad/s]	Hz	-
Mode 1	-0.460 ± j 6.386	1.016	0.0718
Mode 2	-6.121 ± j 9.910	1.577	0.526

Modal analysis does not always support observations from time domain simulations. The intent of adding damping controllers is to increase the damping ratios of critical modes of oscillations. As shown in table 7, results do not align with expectations in this case. Damping of the Mode 1 dropped

from 7.18% to 6.67% and for the Mode 2 the value decreased from 52.6% to 48.2%. The exact reason for such observations of Modal analysis should be investigated in detail to improve the behavior in the future. It is highly possible that such observations made from Modal analysis are connected to an addition of new control loops to the control structures of individual power plants and not spending enough research on correctly tunning the controllers.

TABLE VII.   MODAL ANALYSIS RESULTS WITH DAMPING CONTROLLER

Modes	Eigenvalues	Frequency	Damp. Ratio
Units	[1/s +j rad/s]	Hz	-
Mode 1	-0.427 ± j 6.390	1.017	0.0667
Mode 2	-6.008 ± j 10.91	1.737	0.482
Mode 3	-18.03 ± j 11.58	1.844	0.841

IV. CONCLUSION

The aim of this paper was to evaluate the impacts of Wide Area Monitoring System (WAMS) on grid-forming control with Direct Voltage Control (DVC) and Virtual Synchronous Machine (VSM) and to perform Eigenvalue analysis to evaluate the effect of WAMS on selective damping. This paper assumes that voltage magnitude is a reasonable input for the damping controller and DVC is the controller which is able to receive the signal. Input and output signal selection method was used to determine buses and generators with highest observability and controllability indices. These were used for determining the locations of PMUs and WADCs. Time domain simulations showed enhanced damping in the system with presence of additional damping controllers. A decrease of presence of critical modes of oscillation in the time domain signal was supported by Eigenvalue analysis, however damping did not improve for every critical modes of oscillation. This present opportunity for future research, where control loops of the controllers should be further optimized to allow Eigenvalue analysis to observe results which are in line with time domain simulations. The project was carried out in collaboration with DNV, where the plan is to incorporate the observed information into NextGen GridOps Framework.

V. REFERENCES

[1] M. Ndreko, S. Rüberg and W. Winter, "Grid Forming Control for Stable Power Systems with up to 100 % Inverter Based Generation: A Paradigm Scenario Using the IEEE 118-Bus System," 2018.

[2] V. N. Sewdien, M. van der Meijden, T. Breithaupt, L. Hofmann, D. Herwig, A. Mertens, B. W. Tuinema and J. L. Rueda Torres, "Effects of increasing power electronics on system stability: Results from migrate questionnaire," in *2018 International Conference and Utility Exhibition on Green Energy for Sustainable Development (ICUE)*, 2018.

[3] M. Ndreko , S. Rüberg and W. Winter, "Grid forming control scheme for power systems with up to 100% power electronic interfaced generation: a case study on Great Britain test system," in *Iet Renewable Power Generation*, 2020.

[4] S. V. Dhople, B. B. Johnson and A. O. Hamadeh, "Virtual Oscillator Control for voltage source inverters," in *IEEE Computer Society*, Allerton, 2013.

[5] A. Korai, J. Denecke, J. L. Rueda Torres and E. Rakhshani, "New control approach for blackstart capability of full converter wind turbines with direct voltage control," in *IEEE Milan PowerTech*, Milan, 2019.

[6] M. Younis and R. Iravani, "Wide-area damping control for inter-area oscillations: A comprehensive review," in *2013 IEEE Electrical Power & Energy Conference*, 2013.

[7] J. L. Rueda Torres and I. Erlich, "Input/ouput signal selection for wide-area supplementary damping controllers," in *IFAC Proceedings Volumes*, 2013.

[8] N. Modi, M. Lloyd and T. K. Saha, "Wide-area signal selection for power system damping controller," in *AUPEC*, 2011.

[9] SPEN, GE and UoM, "Deliverable 2.1: Requirements for Monitoring & Forecasting PE-based KPIs," MIGRATE – Massive InteGRATion of power Electronic devices, 2018.

[10] DIgSILENT GmbH, "Description, modelling and simulation of a benchmark system for converter dominated," DIgSILENT GmbH, 2018.

[11] S. D'Arco and J. A. Suul, "Equivalence of virtual synchronous machines and frequency-droops for converter-based microgrids," IEEE Transactions on Smart Grid, 2014.

[12] DIgSILENT GmbH, "Digsilent powerfactory 2021: Technical reference, grid-forming converter templates," DIgSILENT GmbH, 2020.

[13] DIgSILENT GmbH, "39 Bus New England System," DIgSILENT GmbH.

[14] F. M. Gonzalez-Longatt and J. L. Rueda Torres, "Advanced Smart Grid Functionalities Based on PowerFactory," in *Springer International Publishing*, 2018.

[15] DIgSILENT GmbH, "Digsilent powerfactory 2021: User manual," DIgSILENT GmbH, 2020.

[16] A. Akkawi, M. Ali, L. Lamont and L. E. Chaar, Comparative study between various controllers for power system stabilizer using particle swarm optimization, EPECS, 2011.